Heliyon 9 (2023) e13847

Contents lists available at ScienceDirect

Heliyon

journal homepage: www.cell.com/heliyon

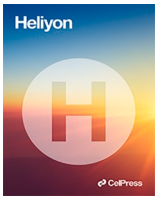

Research article

Chemo-radiation therapy of U87-MG glioblastoma cells using SPIO@AuNP-Cisplatin-Alginate nanocomplex

Mahdie Mousavi [a,b], Fereshteh Koosha [c,*], Ali Neshastehriz [a,b,**]

[a] Radiation Biology Research Center, Iran University of Medical Science (IUMS), Tehran, Iran
[b] Radiation Science Department, Iran University of Medical Science (IUMS), Tehran, Iran
[c] Department of Radiology Technology, school of Allied Medical Sciences, Shahid Beheshti University of Medical Sciences, Tehran, Iran

ARTICLE INFO

Keywords:
Radiotherapy
Chemotherapy
Cisplatin
Gold nanoparticle
Glioma

ABSTRACT

Megavoltage radiotherapy and cisplatin-based chemotherapy are the primary glioblastoma treatments. Novel nanoparticles have been designed to reduce adverse effects and boost therapeutic effectiveness. In the present study, we synthesized the SPIO@AuNP-Cisplatin-Alginate (SACA) nanocomplex, composed of a SPIO core, a gold shell, and an alginate coating. SACA was characterized using transmission electron microscopy (TEM) and dynamic light scattering (DLS). U87-MG human glioblastoma cells and the HGF cell line (a healthy primary gingival fibroblast) were treated in multiple groups by a combination of SACA, cisplatin, and 6 MV X-ray. The MTT assay was used to assess the cytotoxicity of cisplatin and SACA (at various concentrations and for 4 h). Following the treatments, apoptosis and cell viability were evaluated in each treatment group using flow cytometry and the MTT assay, respectively. The findings demonstrated that the combination of SACA and 6 MV X-rays (at the doses of 2 and 4 Gy) drastically decreased the viability of U87MG cells, whereas the viability of HGF cells remained unchanged. Moreover, U87MG cells treated with SACA in combination with radiation exhibited a significant increase in apoptosis, demonstrating that this nanocomplex effectively boosted the radiosensitivity of cancer cells. Even though additional *in vivo* studies are needed, these findings suggest that SACA might be used as a radiosensitizer nanoparticle in the therapy of brain tumors.

1. Introduction

Despite advances in radiotherapy techniques and newly developed chemotherapy and surgery methods in the treatment of glioblastoma multiforme (GBM), the disease does not efficiently respond to treatments, as the median survival of patients undergoing combinational therapy is about 12–15 months [1]. Hypoxia and repopulation of cancerous cells, resistant cancer stem cells, limitations in the delivery of radiation dose to the tumor site, and particularly the problems with the delivery of chemotherapy drugs to GBM cells because of the blood brain barrier (BBB) drew back the treatment of patients with GBM [2,3]. Chemotherapy based on cisplatin is a common first-line treatment for several cancers, including head and neck tumors [4]. Cisplatin has radiosensitizing effects due to the presence of a high atomic number element (platinum) in its structure, inhibiting the post-irradiation DNA damage repair process,

* Corresponding author. Department of Radiology Technology, Faculty of Allied Medical Sciences, Shahid Beheshti University of Medical Sciences, Darband St, Ghods Sq., Tehran, Iran.
** Corresponding author. Radiation Science Department, Iran University of Medical Sciences, Iran.
E-mail addresses: f.koosha@sbmu.ac.ir, frshtkoosha@yahoo.com (F. Koosha), neshastehriz.a@iums.ac.ir (A. Neshastehriz).

https://doi.org/10.1016/j.heliyon.2023.e13847
Received 1 June 2022; Received in revised form 21 January 2023; Accepted 13 February 2023
Available online 17 February 2023

arresting the cell cycle in the G2/M phase, and having the ability to capture and transfer radicals and low-energy electrons induced by radiation to guanine bases in DNA to produce significant DNA double-strand breaks (DSBs) [5,6]. On the other hand, systematic distribution of chemotherapeutics in the body causes multiple complications in healthy tissues and induces unwanted side effects, including nausea, vomiting, decreased blood cells, kidney, and nervous system damage, as well as hair loss in patients [7]. Limitations in the treatment of GBM as a resistant tumor model led researchers to take advantage of nanoparticles (NPs) in cancer treatment studies. NPs are smaller than 1000 nm in size and possess special properties that must be tuned up in terms of size, shape, coating with functional groups, targeting cancer cells, being used as drug carriers, photothermal agents, imaging contrast agents, and radiosensitizers [8,9]. In recent years, multiple studies have suggested that administration of gold nanoparticles (AuNP) into tumors may improve radiosensitivity [10–14]. When irradiated by X-ray, AuNPs (with a high atomic number and high photon absorption cross-section) are able to generate numerous low-energy electrons and free radicals, resulting in a higher rate of cell death and apoptosis [15,16].

As another type of NP, superparamagnetic iron oxide (SPIO) has recently opened up a new window to the diagnosis and treatment of cancer [17–20]. In addition to its good capabilities in cancer magnetic resonance imaging (MRI), the ability of SPIO to cross the BBB and remain in the lesion is one of its properties worth considering in the field of cancer treatment [21]. According to the above-mentioned properties of AuNPs, SPIOs, and cisplatin, here we propose a new polymeric nanocomposite containing cisplatin and the nano-scaled core-shell structure of SPIO@AuNP. We incorporated these components into a polymeric matrix made of alginate to form the SPIO@AuNP-Cisplatin-Alginate nanocomplex, or SACA for short. We chose alginate to make such a polymeric nanocomposite because it is a natural and non-toxic polymer and it can enhance the solubility and stability of the NPs in physiological conditions [22]. Multiple studies have been published so far on the radiosensitizing effects of cisplatin, SPIOs, AuNPs, and SPIO@AuNP core-shell nanostructures [17,23,24]. The aim of the present study was to investigate the radiosensitizing effects of an all-in-one nanocomposite (like SACA) when human glioma U87-MG cells and healthy primary gingival fibroblast HGF cells are irradiated by megavoltage X-rays *in vitro*.

2. Materials and methods

2.1. SACA nanocomplex preparation

The SPIO@AuNP-Cisplatin-Alginate (SACA) nanocomplex was prepared as previously described [17,25–27]. Using a modified version of Massart's co-precipitation method, Fe_3O_4 NPs were synthesized [28]. A solution containing iron (II) and iron (III) in a molar ratio of 1:2 was immediately given 12 mL of ammonia. The precipitated black Fe_3O_4 NPs were then re-dispersed in toluene after being washed three times with methanol. Then 12.5 mL of Fe_3O_4 and 0.025 mL of 3-Aminopropyl trimethoxysilane (APTMS) were combined and sonicated for 30 min. Magnet separation, methanol washing, and methanol dispersion were all used to separate the precipitate. The Jana et al. approach [29] was used to manufacture AuNPs (3.5 nm in diameter), which were then adsorbed onto the surface of APTMS-functionalized Fe_3O_4 NPs to create the gold shell on the surface of the Fe_3O_4 NPs core. To this end, a 0.02 g solution of APTMS-functionalized Fe_3O_4 NPs in methanol was gently added to a 20 mL colloidal solution of AuNPs. Au shell was formed primarily after 2 h of stirring at room temperature. The resultant NPs were magnetically separated, thoroughly washed with distilled water three times, and then resuspended in 15 mL of distilled water. Under sonication, a weak redactor (a solution of chloroauric acid) and ascorbic acid were added to the above solution to finish making the Au shell. The Fe_3O_4@Au NPs were separated using a magnet and washed three times with distilled water after being stirred at room temperature for 2 h. The surface modification agent was then sodium alginate (2%). For this, the NPs solution was rapidly stirred in diluted sodium alginate (2%) at room temperature for 2 h in the dark. After that, a magnetic stirrer running at 800 rpm at room temperature was used to mix the Fe_3O_4@AuNP-alginate hydrogel very well as cisplatin solution was added drop by drop to a final concentration of 50 ppm. The synthesis procedure of SACA nanocomposite is

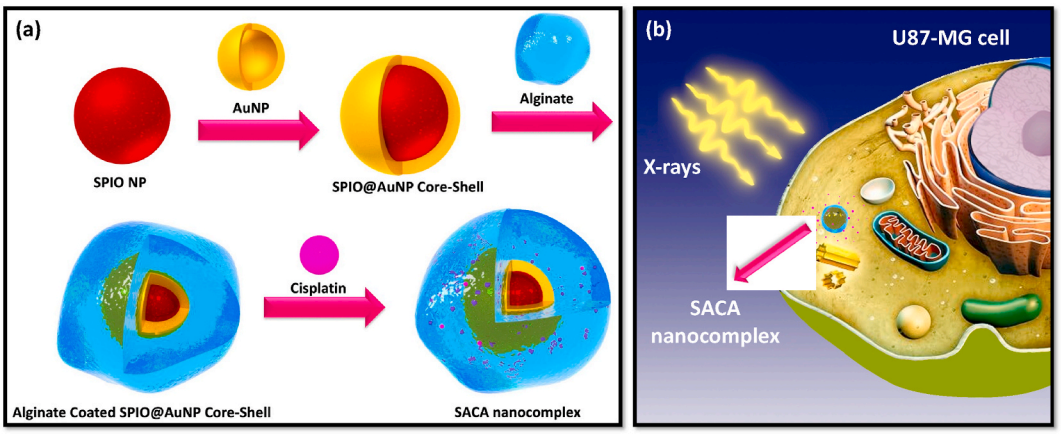

Fig. 1. (a) The SACA nanocomplex synthesis procedure and (b) its application in the chemo-radiation therapy of brain cancer.

demonstrated in Fig. 1. Cell culture medium, Dulbecco's Modified Eagle Medium (DMEM), penicillin-streptomycin and Trypsin-EDTA were purchased from Sigma-Aldrich Corp. (St. Louis, MO, USA). Fetal bovine serum (FBS) was purchased from Gibco® (USA). 3-(4, 5-dimethylthiazol-2-yl)-2,5-diphenyltetrazolium bromide (MTT) cell proliferation assay kit were obtained from Sigma (San Diego, CA) and a flow cytometry kit was purchased from eBioscience (San Diego, CA).

2.2. SACA nanocomplex characterization

The morphology and size distribution of the synthesized nanocapsules were analyzed by transmission electron microscopy (TEM; LEO906-ZEISS, Germany). Also, the Malvern Zetasizer Nano ZS-90 instrument was used to measure the hydrodynamic diameter and Zeta potential distribution of the nanocapsules that had been made. The release profile of the SACA nanocomplex has been measured in our previous studies [25–27].

2.3. Cell culture

U87-MG and HGF cell lines were purchased from the Pasteur Institute of Iran (Tehran, Iran). The cells were routinely cultured in DMEM medium supplemented with 10% heat-inactivated fetal bovine serum, 100 U/mL penicillin, and 100 mg/mL streptomycin in a humidified atmosphere with 5% CO2 at 37 °C. The culture medium was refreshed every 2 days.

2.4. Cytotoxicity effects of cisplatin and SACA

A microculture tetrazolium assay (MTT) was applied to evaluate the cytotoxicity of cisplatin and SACA. The cells were cultured at a density of 1×10^4 cells per well in 96-well plates. After reaching cells at about 90% confluency, the medium of each well was changed, and cisplatin and SACA were added at different concentrations and incubated for 4 h at the standard conditions. Based on the pilot studies and previous experiments with the SPIO@AuNP-Alginate nanocomplex [25–27], we chose 4 h of incubation. Tests were repeated in six wells for each concentration and incubated for 4 h. Instantly thereafter, the percentage of cell death is evaluated using the MTT assay. All experiments were repeated at least three times.

2.5. Evaluating cytotoxic effects of cisplatin and SACA in combination with radiotherapy

After determining the optimal concentration of cisplatin and SACA nanocapsule, cells were irradiated at optimal drug doses with distinct doses of 6 MV X-ray. Investigating the radiosensitization of SACA and cisplatin, the cells were seeded in a 96-well cell culture plate at a density of 1×10^4 cells per well. After 24 h, the indicated agents, cisplatin and SACA, were added to each well at a concentration of 5 μg/mL and 30 μg/mL respectively. The wells were washed with phosphate buffered saline (PBS) after 4 h. Immediately afterward, plates were irradiated with two doses of 6 MV X-ray (2 and 4 Gy) by an Elekta linear accelerator (Stockholm, Sweden) at a dose rate of 2 Gy/min. The flasks were irradiated at the field size of 10*10 cm^2 from the posterior at an SSD (source-to-skin distance) of 100 cm. MTT assay and flow cytometry were accomplished to investigate the effects of combined therapies.

2.6. MTT assay

To perform the MTT assay, briefly, U87MG and HGF cells were seeded at a density of 10,000/well into a 96-well culture plate and incubated with the agents for 4 h. After removing the media and washing each well 3 times with PBS, the cells were further incubated with 100 μL of MTT solution at 37 °C for 4 h. The resulting formazan was solubilized with DMSO, and the absorption was measured at 570 nm in an ELISA reader (DYNEX MRX, USA).

2.7. Flow cytometry assay

To investigate the effect of combinational treatment with cisplatin, SACA and radiotherapy on the induction of apoptosis, cells were seeded into 12-well plates, and following various treatments, measurements were performed by propidium iodide (PI) staining and flow cytometry analysis. Annexin-V-Flous (5 μl per sample) was added, and cell suspensions were incubated for 20 min in the dark. Finally, 5 μl of PI was added to the sample, and fluorescence was measured using flow cytometry. Annexin V-positive and PI-negative cells were considered to be in the early apoptotic phase, and cells having positive staining for both Annexin-V and PI were considered to undergo late apoptosis or necrosis.

2.8. Statistical analysis

Experimental data are presented as mean ± standard deviation (SD) of three independent experiments. All tests were done in triplicate. For statistical analysis, a one-way ANOVA was performed using GraphPad Prism 6 software, followed by Tukey's test as the post-hoc analysis. The value of $p < 0.05$ was considered to be statistically significant.

3. Results

3.1. Nanoparticle characterization results

Fig. 2 (a) depicts a TEM image of the SACA nanocapsule, which clearly shows the surface morphology of SACA with its spherical structure. According to Fig. 2 (b), the hydrodynamic diameter of the SACA was measured in the range of 40–100 nm, with the highest frequency occurring at 58 ± 10 nm. The fact that the Zeta potential of the SACA nanocapsule was −18 ± 2 mV supports that the SACA nanocapsule had acceptable stability (Fig. 2(c)). Further information on NP characterizations has been reported in our previous publications [25–27].

3.2. Cytotoxicity effects of cisplatin and SACA nanocapsule

To assess the cytotoxicity of cisplatin and the SACA nanocomplex, U87MG and HGF, as malignant and healthy cell lines, respectively, were treated with different concentrations of the determined agents. The MTT assay results revealed that increasing the concentration of each drug significantly reduced cell viability in both treated cell lines (Fig. 3(a) and (b)). Based on Fig. 3, the IC50 values for cisplatin and nanocomplex have been calculated to be 81.9 ± 8.2 μg/mL and 133.3 ± 13.5 μg/mL respectively. Moreover, according to the viabilities in various concentrations, cisplatin and SACA with the doses of 5 μg/mL and 30 μg/mL respectively, have been selected as optimal doses for the rest of the experiments. Selected concentrations of cisplatin and SACA did not cause significant toxicity compared to the control group, and the degree of toxicity was almost the same in both cell lines.

3.3. Radiosensitization effects of cisplatin

To investigate the radiosensitizing effect of cisplatin, U87MG and HGF cells were incubated with cisplatin at a concentration of 5 μg/mL for 4 h and then exposed to 2 and 4 Gy of 6 MV X-ray. After 24 h cell viability was measured using MTT assay. Cisplatin combined with radiation significantly increased cell death compared to cisplatin alone, as shown in Fig. 3(c). Also, Fig. 3(c) demonstrates that the viability of the U87MG cells that received cisplatin alone or in combination with radiation at the dose of 2 Gy is 92.6% and 73.8%, respectively. Furthermore, the results show that at a dose of 2 Gy, the viability of HGF cells decreased significantly.

3.4. Radiosensitization effects of SACA nanocapsule

The radiosensitization of SACA nanocapsules at a concentration of 30 μg/mL following 4 h of incubation was assessed after irradiation. The MTT assay was performed 24 h after radiation therapy. As presented in Fig. 3(d), the viability of the U87MG cells treated with SACA nanocapsule combined with 2 Gy X-ray was significantly lower compared to SACA nanocapsule alone ($p < 0.05$), while for the HGF cells, the viability difference between the two mentioned groups was not significant ($p > 0.05$).

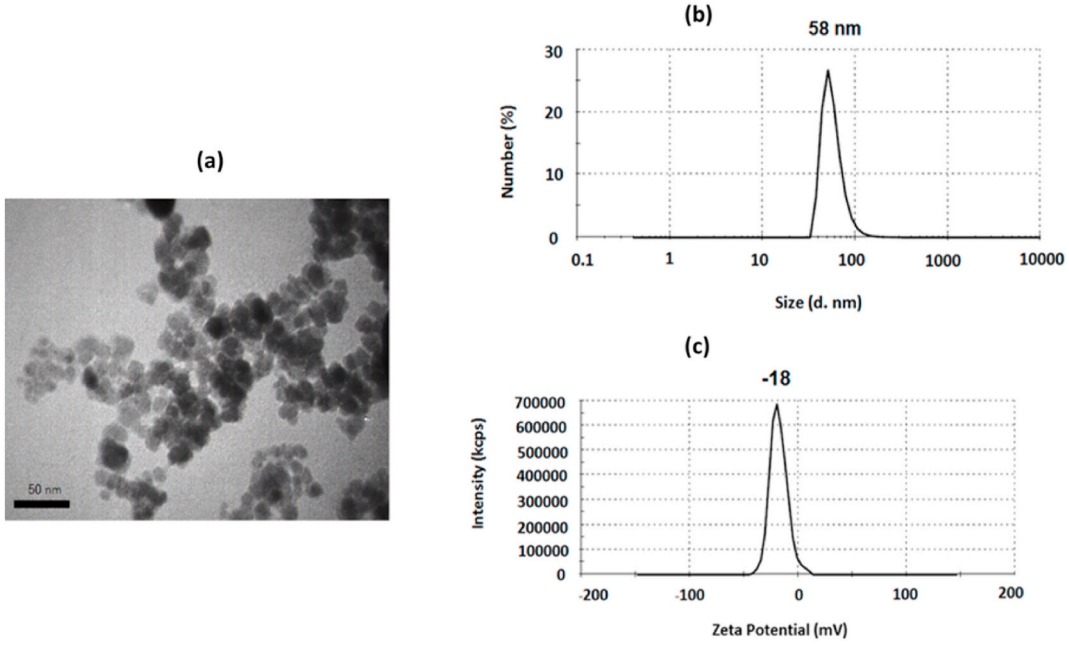

Fig. 2. (a) Transmission electron microscopy (TEM) image of the synthesized nanocomplex, (b) Hydrodynamic size (DLS) distribution of the synthesized nanocomplex, and (c) The Zeta potential profile of the synthesized nanocomplex.

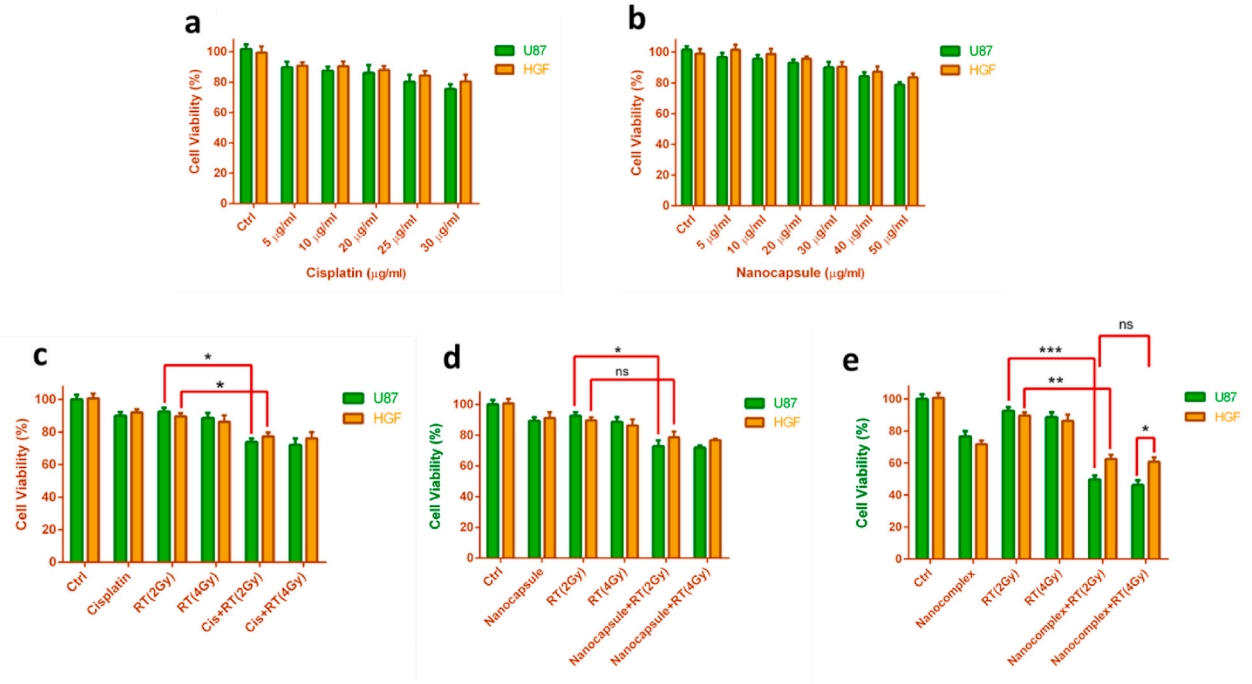

Fig. 3. (a) The viability of U87-MG and HGF cells treated with different concentrations of cisplatin. (b) The viability of U87-MG and HGF cells treated with different concentrations of nanocapsule. (c) The viability of U87-MG and HGF cells treated with cisplatin and then exposed to different doses of X-ray radiation (ns stands for not statistically significant, *$p < 0.05$, **$p < 0.01$, and ***$p < 0.001$ when each experimental group was compared with its corresponding control group), (d) The viability of U87-MG and HGF cells treated with nanocapsule and then exposed to different doses of X-ray radiation (ns stands for not statistically significant, *$p < 0.05$, **$p < 0.01$, and ***$p < 0.001$ when each experimental group was compared with its corresponding Control group), (e) the viability of U87-MG and HGF cells received combination therapy of nanocomplex (incubated for 4 h) and radiation; 2 Gy and 4 Gy. (ns stands for not statistically significant, *$p < 0.05$, **$p < 0.01$, and ***$p < 0.001$ when each experimental group was compared with its corresponding control group).

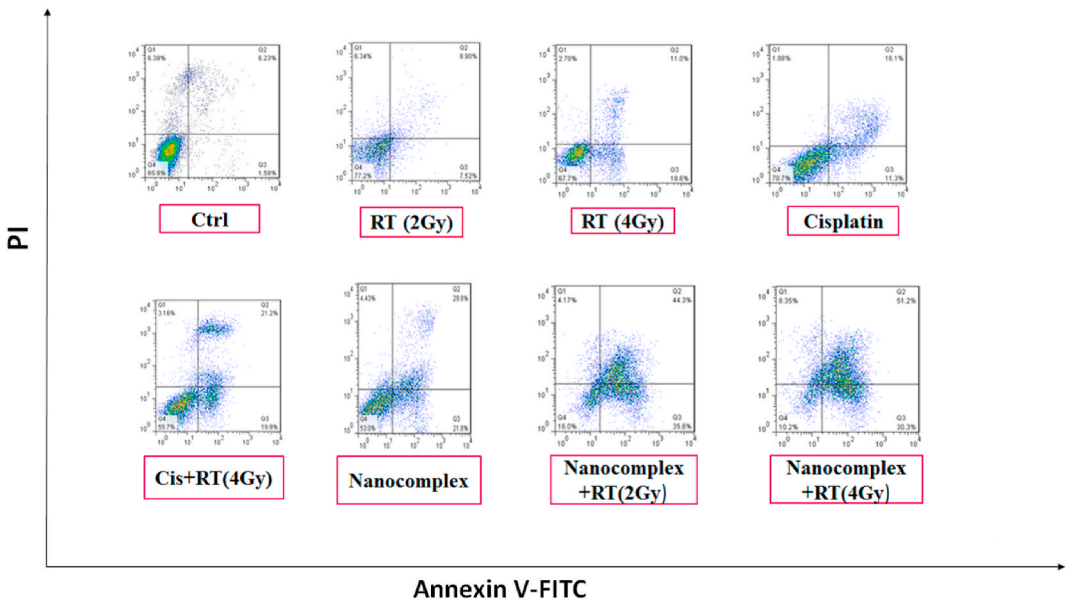

Fig. 4. Flow cytometry results obtained after various combinatorial treatments for U87MG cells. In each panel, Q1 shows necrotic cells, Q2 shows later period apoptotic cells, Q3 shows normal cells and the Q4 shows early apoptotic cells.

3.5. Radiosensitization effects of SACA nanocomplex

Further, the therapeutic efficacy of the SACA nanocomplex was evaluated after 4 h of incubation and irradiation with X-ray on both cell lines using the MTT assay. According to Fig. 3(e), the viability of the U87MG cells after receiving the SACA nanocomplex alone or in combination with 2 Gy of radiation is 76.5% and 49.6%, respectively. It can be seen that radiosensitization of the SACA nanocomplex increased significantly in U87MG cells when compared to cells treated only with radiation. Interestingly, the viability of HGF cells remains constant across both doses of 6 MV X-ray tested.

3.6. Apoptosis analysis

Induction of apoptosis in multiple treatment groups was evaluated on U87MG cells and HGF cells. The results of annexin V/PI flow cytometry are shown in Figs. 4–6. Based on our results, in both cell lines treated with 2 and 4 Gy of X-ray alone, no considerable apoptosis was seen compared to the control group, and it can also be seen that for the HGF cell line, apoptosis remained constant. Further, the SACA nanocomplex alone statistically increased apoptosis compared to the control and cisplatin groups ($P < 0.05$). The number of U87MG cells that died due to apoptosis was much higher in the group that was treated with SACA nanocomplex and 6 MV X-ray (4 Gy) than in the group that was only treated with radiation (81.5% vs. 29.6%). However, in the HGF cell line, the apoptosis rate was remarkably lower than that of U87MG cells in combinational treatment groups.

4. Discussion

Cisplatin is among the major chemotherapy drugs with the ability to crosslink DNA and induce apoptosis by activating various signal transduction pathways. This chemotherapy agent has many side effects because it is so toxic to the whole body. These include kidney toxicity, nerve toxicity, and ear toxicity [30,31]. To get around the fact that chemotherapeutic drugs can be harmful to the whole body, many nanoparticle-based platforms have been made to deliver drugs only to the tumor by using both passive and active targeting [32,33]. Conjugating gold nanoparticles with anti-cancer agents may improve the pharmacokinetics and anti-cancer efficiency of the drugs and consequently minimize their adverse effects. Also, the radiosensitizing effect of high Z nanoparticles could effectively enhance the therapeutic efficacy of radiotherapy treatment of tumors. In our previous studies, we showed that gold-coated iron oxide nanoparticles (Au@Fe_2O_3) enhanced radiosensitization of KB cells. In the present study, a unique nanocomplex has been synthesized that combines both radiosensitization and targeted drug delivery abilities, which can significantly enhance the therapeutic effect and treatment outcomes. The SACA nanocomplex is composed of SPIO with a gold shell coated with alginate and, as a carrier, delivers cisplatin to the U87MG tumor cells and HGF cells as a healthy cell line.

As shown in Fig. 2, the SACA nanocapsule is spherical in shape, and the size of the nanocapsule is about 58 nm. HR-TEM and UV–Vis spectra of nanoparticles confirmed the formation of a core-shell structure. It was also found that the zeta potential of a nanocapsule is −18 mV, and such a potential seems to be acceptable for having a sample of stable nanocapsules. The alginate that we used as a coating material is highly biocompatible, low-toxic, and cost-effective. These characteristics make it very appropriate for biomedical

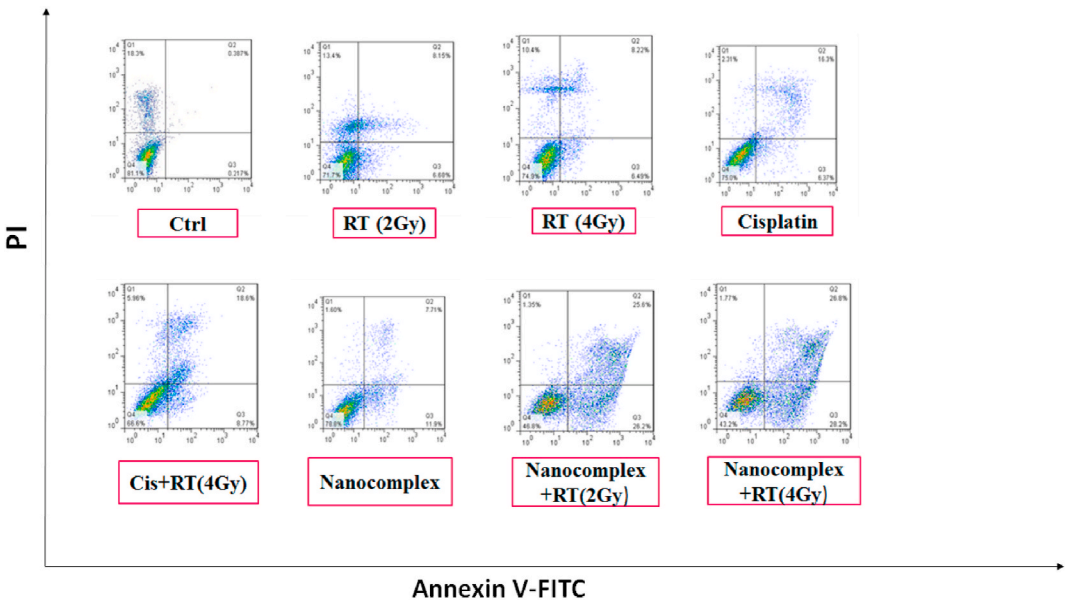

Fig. 5. Flow cytometry results obtained after various combinatorial treatments for HGF cells. In each panel, Q1 shows necrotic cells, Q2 shows later period apoptotic cells, Q3 shows normal cells and the Q4 shows early apoptotic cells.

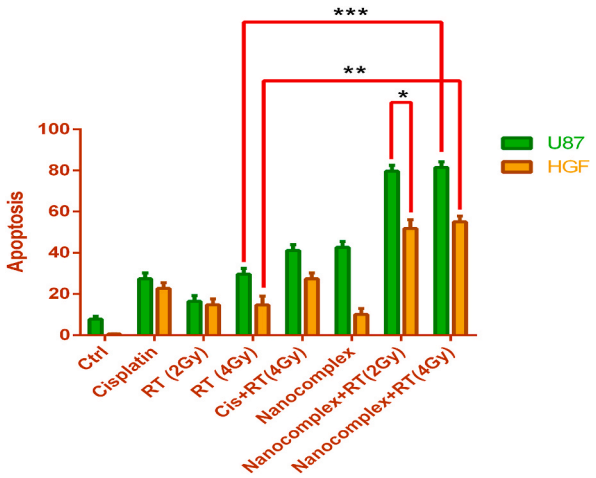

Fig. 6. Percentage of apoptosis in U87MG and HGF cell lines after receiving various treatment regimens (ns stands for not statistically significant, *p < 0.05, **p < 0.01, and ***p < 0.001 when each experimental group was compared with its corresponding control group).

applications [34]. Moreover, experiments revealed that alginate has a rare interaction with proteins, which decreases the capture of alginate-based systems by macrophages and can be utilized as a delivery vehicle in cancer therapeutic methods [35]. Further, alginate can extend the blood circulation time of nanocarriers and prevent them from rapid body clearance [36,37]. As shown in Fig. 3, treating U87MG and HGF cells with cisplatin and nanocapsule dosage decreased the viability of U87MG cells in a dose-dependent manner. Accordingly, in this *in vitro* experiment, concentrations of 5 μg/mL and 30 μg/mL of cisplatin and SACA, respectively, demonstrated minimum toxicity on HGF and U87MG cell lines and were utilized for multiple treatments. We showed that both cisplatin and nanocapsules in determined concentrations enhanced radiosensitization of U87MG cells, but nanocapsules showed a selective attitude toward healthy and tumoral cell lines at the dose of 2 Gy (Fig. 3(d)). It may be due to the cellular structure of healthy cells that limits the permeability of nanocapsules through the cell membrane. Also, it is known that because of the enhanced permeability and retention (EPR) effect, molecules of certain sizes (typically liposomes, nanoparticles, and macromolecular drugs) tend to accumulate in tumor tissue much more than they do in normal tissues [38]. Moreover, SACA nanocomplex potentially radiosensitized U87MG cells, as it can be seen in Figure 3(e), where the percentage of cell death was higher in U87MG cells treated with SACA nanocomplex at the dose of 2 Gy in comparison with tumor cells treated with 2 Gy alone, and this reduction in cell death is more significant in U87MG cells in similar groups. The SACA nanocomplex could make cells more sensitive to radiation by making ROS, causing DNA damage, and stopping DNA repair. Also, the presence of Au ($z = 79$) and platinum ($z = 78$) in SACA can physically enhance the radiation dose by the emission of secondary ionizing radiation (Auger/photo electrons) [5]. Additionally, we found that combining cisplatin with radiation drastically reduced cell survival and induced apoptosis. Accordingly, our results of annexin V/PI analysis (Figs. 4 and 5) confirmed the apoptotic death in the multiple treatment groups. Apoptosis is one of the main consequences following combinational therapy with SACA, as it is demonstrated in Fig. 4. SACA combined with 6 MV X-ray significantly increased the apoptosis percentage in U87MG cells. Moreover, the apoptosis percentage of U87MG cells is significantly higher than HGF cells in groups treated with nanocomplex and radiotherapy, indicating that SACA is a potent radiosensitizer for megavoltage X-rays as used in external beam radiotherapy. Moreover, our data showed that the SACA nanocomplex alone has the ability to increase apoptosis in U87MG cells. The results show that chemoradiation therapy could control tumors better than each method alone by making radioresistant hypoxic cells more vulnerable, stopping the repair of sub-lethal damage caused by radiation, and stopping the cell cycle in radiosensitive G2/M phases [39]. In accordance with our study, Davidi et al. synthesized 20 nm gold nanoparticles coated with glucose and cisplatin (CG-GNPs) and investigated their chemo-radiosensitization on A431 cells. They found out that their synthesized nanoparticles have a great potential to increase antitumor effects and overcome resistance to chemotherapeutics and radiation [40]. Alamzadeh et al. investigated the radiosensitization of Au@Alg nanoparticles (ACA) (co–loaded with cisplatin) combined with 6 MV X-ray against KB human mouth epidermal carcinoma cells. Their results showed a higher cytotoxicity of their designed nanocomplex combined with radiation than applying ACA and radiotherapy individually, which indicated the chemo-radiosensitizing effect of this nanocomplex [41]. Thus, the synthesized SACA obtained by applying the SPIO core, gold shell, and alginate coating could efficiently radiosensitize GBM cells and enhance the therapeutic efficiency. We showed that the chemotherapy drug cisplatin inside a nanocapsule could cause apoptosis in tumor cells much more than in a healthy HGF cell line.

In this work, we synthesized the SACA nanocomplex and examined its ability to radiosensitize human glioma cells *in vitro*. Our nanocomplex characterization results showed that SACA has a spherical structure and acceptable stability. Notably, we found that SACA increased apoptosis and markedly decreased survival in the U87MG cell line compared to HGF cells, which were irradiated by 6 MV X-ray. Hence, it can be concluded that SACA may enhance the radiation effect in radiotherapy of U87MG cells with megavoltage energies and have less effect on HGF normal cells. In the near future, more investigation into the therapeutic efficacy of this nanocomplex will be needed in *in vivo* experiments.

Author contribution statement

Mahdie Mousavi: Performed the experiments; Analyzed and interpreted the data; Contributed reagents, materials, analysis tools or data; Wrote the paper. Fereshteh Koosha: Conceived and designed the experiments; Performed the experiments; Analyzed and interpreted the data; Contributed reagents, materials, analysis tools or data; Wrote the paper. Ali Neshastehriz: Conceived and designed the experiments; Analyzed and interpreted the data; Wrote the paper.

Funding statement

This research was supported by Iran University of Medical Sciences.

Data availability statement

Data will be made available on request.

Declaration of competing interest

The authors declare no competing interests.

References

[1] O. Van Tellingen, et al., Overcoming the blood–brain tumor barrier for effective glioblastoma treatment, Drug Resist. Updates 19 (2015) 1–12.
[2] J. Mann, et al., Advances in radiotherapy for glioblastoma, Front. Neurol. 8 (2018) 748.
[3] A. Popovtzer, et al., Actively targeted gold nanoparticles as novel radiosensitizer agents: an in vivo head and neck cancer model, Nanoscale 8 (5) (2016) 2678–2685.
[4] D. Rades, et al., Comparing two lower-dose cisplatin programs for radio-chemotherapy of locally advanced head-and-neck cancers, Eur. Arch. Oto-Rhino-Laryngol. 274 (2) (2017) 1021–1027.
[5] L. Cui, et al., Significant radiation enhancement effects by gold nanoparticles in combination with cisplatin in triple negative breast cancer cells and tumor xenografts, Radiat. Res. 187 (2) (2017) 147–160.
[6] Q.-B. Lu, S. Kalantari, C.-R. Wang, Electron transfer reaction mechanism of cisplatin with DNA at the molecular level, Mol. Pharm. 4 (4) (2007) 624–628.
[7] V. Schirrmacher, From chemotherapy to biological therapy: a review of novel concepts to reduce the side effects of systemic cancer treatment, Int. J. Oncol. 54 (2) (2019) 407–419.
[8] M. Mirrahimi, et al., A thermo-responsive alginate nanogel platform co-loaded with gold nanoparticles and cisplatin for combined cancer chemo-photothermal therapy, Pharmacol. Res. 143 (2019) 178.
[9] X. Bai, et al., The basic properties of gold nanoparticles and their applications in tumor diagnosis and treatment, Int. J. Mol. Sci. 21 (7) (2020) 2480.
[10] M.M. Movahedi, et al., Investigating the photo-thermo-radiosensitization effects of folate-conjugated gold nanorods on KB nasopharyngeal carcinoma cells, Photodiagnosis Photodyn. Ther. 24 (2018) 324–331.
[11] S. Khademi, et al., Evaluation of size, morphology, concentration, and surface effect of gold nanoparticles on X-ray attenuation in computed tomography, Phys. Med. 45 (2018) 127–133.
[12] A. Shakeri-Zadeh, et al., Gold nanoparticles conjugated with folic acid using mercaptohexanol as the linker, Journal Nanotechnology Progress International 1 (1) (2009) 1–44.
[13] A. Hashemian, et al., Folate-conjugated gold nanoparticles (synthesis, characterization and design for cancer cells nanotechnology-based targeting), Int. J. Nanosci. Nanotechnol. 5 (1) (2009) 25–34.
[14] J. Beik, et al., Gold nanoparticle-induced sonosensitization enhances the antitumor activity of ultrasound in colon tumor-bearing mice, Med. Phys. 45 (9) (2018) 4306–4314.
[15] S. Her, D.A. Jaffray, C. Allen, Gold nanoparticles for applications in cancer radiotherapy: mechanisms and recent advancements, Adv. Drug Deliv. Rev. 109 (2017) 84–101.
[16] K. Haume, et al., Gold nanoparticles for cancer radiotherapy: a review, Cancer nanotechnology 7 (1) (2016) 8.
[17] A. Neshastehriz, et al., Gold-coated iron oxide nanoparticles trigger apoptosis in the process of thermo-radiotherapy of U87-MG human glioma cells, Radiat. Environ. Biophys. 57 (4) (2018) 405–418.
[18] Z. Abed, et al., Iron oxide–gold core–shell nano-theranostic for magnetically targeted photothermal therapy under magnetic resonance imaging guidance, J. Cancer Res. Clin. Oncol. 145 (5) (2019) 1213–1219.
[19] J. Beik, et al., Simulation-guided photothermal therapy using MRI-traceable iron oxide-gold nanoparticle, J. Photochem. Photobiol. B Biol. 199 (2019), 111599.
[20] M. Asadi, et al., MRI-based numerical modeling strategy for simulation and treatment planning of nanoparticle-assisted photothermal therapy, Phys. Med. 66 (2019) 124.
[21] H. Maeda, G. Bharate, J. Daruwalla, Polymeric drugs for efficient tumor-targeted drug delivery based on EPR-effect, Eur. J. Pharm. Biopharm. 71 (3) (2009) 409–419.
[22] A. Sood, et al., Multifunctional gold coated iron oxide core-shell nanoparticles stabilized using thiolated sodium alginate for biomedical applications, Mater. Sci. Eng. C 80 (2017) 274–281.
[23] B.L. Ferreira, et al., Nanostructured functionalized magnetic platforms for the sustained delivery of cisplatin: synthesis, characterization and in vitro cytotoxicity evaluation, J. Inorg. Biochem. 213 (2020), 111258.
[24] M. Khafaji, M. Zamani, M. Vossoughi, Doxorubicin/cisplatin-loaded superparamagnetic nanoparticles as A stimuli-responsive Co-delivery system for chemo-photothermal therapy, Int. J. Nanomed. 14 (2019) 8769.
[25] A. Neshastehriz, et al., Investigating the therapeutic effects of alginate nanogel co-loaded with gold nanoparticles and cisplatin on U87-MG human glioblastoma cells, Anti Cancer Agents Med. Chem. 18 (6) (2018) 882–890.
[26] M. Keshavarz, et al., Alginate hydrogel co-loaded with cisplatin and gold nanoparticles for computed tomography image-guided chemotherapy, J. Biomater. Appl. 33 (2) (2018) 161–169.
[27] A. Safari, et al., Optimal scheduling of the nanoparticle-mediated cancer photo-thermo-radiotherapy, Photodiagnosis Photodyn. Ther. 32 (2020), 102061.
[28] R. Massart, Preparation of aqueous magnetic liquids in alkaline and acidic media, IEEE Trans. Magn. 17 (2) (1981) 1247–1248.
[29] N.R. Jana, L. Gearheart, C.J. Murphy, Seeding growth for size control of 5– 40 nm diameter gold nanoparticles, Langmuir 17 (22) (2001) 6782–6786.
[30] A.-M. Florea, D. Büsselberg, Cisplatin as an anti-tumor drug: cellular mechanisms of activity, drug resistance and induced side effects, Cancers 3 (1) (2011) 1351–1371.

[31] S. Dhar, et al., Targeted delivery of cisplatin to prostate cancer cells by aptamer functionalized Pt (IV) prodrug-PLGA–PEG nanoparticles, Proc. Natl. Acad. Sci. USA 105 (45) (2008) 17356–17361.
[32] E.A. Murphy, et al., Nanoparticle-mediated drug delivery to tumor vasculature suppresses metastasis, Proc. Natl. Acad. Sci. USA 105 (27) (2008) 9343–9348.
[33] T. Dreifuss, et al., Theranostic gold nanoparticles for CT imaging, in: Design and Applications of Nanoparticles in Biomedical Imaging, Springer, 2017, pp. 403–427.
[34] K.Y. Lee, D.J. Mooney, Alginate: properties and biomedical applications, Prog. Polym. Sci. 37 (1) (2012) 106–126.
[35] D.-G. Ahn, et al., Doxorubicin-loaded alginate-g-poly (N-isopropylacrylamide) micelles for cancer imaging and therapy, ACS Appl. Mater. Interfaces 6 (24) (2014) 22069–22077.
[36] W. Feng, et al., Effect of pH-responsive alginate/chitosan multilayers coating on delivery efficiency, cellular uptake and biodistribution of mesoporous silica nanoparticles based nanocarriers, ACS Appl. Mater. Interfaces 6 (11) (2014) 8447–8460.
[37] M. Mirrahimi, et al., Enhancement of chemoradiation by co-incorporation of gold nanoparticles and cisplatin into alginate hydrogel, J. Biomed. Mater. Res. B Appl. Biomater. 107 (8) (2019) 2658–2663.
[38] A. Nel, E. Ruoslahti, H. Meng, New Insights into “Permeability” as in the Enhanced Permeability and Retention Effect of Cancer Nanotherapeutics, ACS Publications, 2017.
[39] M. Toulany, et al., Cisplatin-mediated radiosensitization of non-small cell lung cancer cells is stimulated by ATM inhibition, Radiother. Oncol. 111 (2) (2014) 228–236.
[40] E.S. Davidi, et al., Cisplatin-conjugated gold nanoparticles as a theranostic agent for head and neck cancer, Head Neck 40 (1) (2018) 70–78.
[41] Z. Alamzadeh, et al., Gold nanoparticles promote a multimodal synergistic cancer therapy strategy by co-delivery of thermo-chemo-radio therapy, Eur. J. Pharmaceut. Sci. 145 (2020), 105235.